Amyloids

DOI: 10.1002/anie.201008276

The Amyloid–Congo Red Interface at Atomic Resolution**

Anne K. Schütz, Alice Soragni, Simone Hornemann, Adriano Aguzzi, Matthias Ernst, Anja Böckmann, and Beat H. Meier**

Amyloids are β-sheet-rich proteinaceous aggregates that are a pathological hallmark of a number of human diseases.[1] They can replicate by seeded nucleation and propagate as prions, and may even exert important physiological activities.[2] Amyloids are universally defined by their stainability with Congo red and the resulting green birefringence.[3] Yet, remarkably, the binding mechanism, geometry, and fine structure of the Congo red/amyloid complex are not known. By using solid-state NMR spectroscopy we have characterized, at atomic resolution, the binding interface between Congo red and amyloid fibrils formed by the prion domain of the fungal HET-s protein.[4] The dye binds highly site-specifically by interacting with residues flanking a groove in the vicinity of a β-arc. The three-dimensional (3D) structure of the fibril is strongly conserved upon the binding of Congo red. Remarkably, a single point mutation, designed according to the binding information, provides an artificial amyloid structurally indistinguishable from HET-s but not stainable by Congo red. The methods used require no isotope labeling of the small molecule and can be used to characterize the interaction of a broad range of dyes, drugs, and tracers with amyloids or other insoluble proteins.

Congo red (Figure S1 in the Supporting Information) is a small molecule that reacts specifically with amyloids and has been used since the 1920s[5] as the analytical "gold standard" for amyloid characterization and diagnostics.[6] Despite its binding specificity and its antiamyloidogenic properties, the use of Congo red as a molecular amyloid tracer in vivo[7] and as an antiamyloid drug[8] has been hindered by its high toxicity and poor pharmacokinetics. Contradictory reports exist on the nature of the interaction between Congo red and amyloid fibrils, but the following facts are generally agreed upon: Congo red binds roughly stochiometrically,[6d,9] and the bound form displays a characteristic red-shift in its absorbance maximum, and shows dichroism and birefringence.[6a,10] The negatively charged sulfate groups of Congo red are believed to be relevant for binding to two sites separated by a distance of approximately 20 Å.[11] In the absence of atomic-resolution structure information, the binding mode is still debated. The long axis of the dye has been postulated to orient parallel or perpendicular to the fibril axis, and the dye binds as a monomer, oligomer, or micelle,[6c,d] or intercalated between the β-sheets.[6c,12] Hydrogen bonds and hydrophobic, aromatic, and ionic interactions have been assumed to contribute to the binding of Congo red to amyloid fibrils.[6d] Also, different side chains from residues such as histidine,[13] arginine,[13b] and lysine[9] have been suspected to promote congophilia.

Atomic-resolution structures of amyloids, which have become available recently, enable studies of the interplay between these proteins and their binding partners in detail. HET-s(218–289), the prion-forming domain of the HET-s prion from the filamentous fungus *Podospora anserina*, is presently one of the structurally most precisely defined amyloids.[4b]

To identify the protein surface that interacts with binding partners by NMR spectroscopy, we set out to detect characteristic chemical-shift perturbations (CSP)[14] upon binding by comparing two-dimensional (2D) ^{13}C–^{13}C correlation spectra (proton-driven spin diffusion, PDSD) of stained and unstained [^{13}C,^{15}N]-labeled fibrils. Since CSPs can be allosteric, we also performed polarization-transfer (PT) experiments which directly probe the spatial proximity of ligand and protein by exploiting the pronounced distance dependence (r^{-3}) of the dipolar interaction. Previously published PT approches[15] have proven difficult for our system as they require isotope-labeled Congo red. We have therefore devised a method relying on polarization transfer from ligand ^{1}H atoms to protein ^{13}C atoms, which uses standard [^{2}H,^{13}C,^{15}N]-isotope-labeled protein but does not require isotopically labeled ligand. In such samples, the protons from Congo red are the unique polarization source in ^{1}H–^{13}C polarization-transfer experiments, and the ^{13}C signals detected identify residues in spatial proximity to Congo red (< 4 Å). For enhanced spectral resolution, the ^{13}C atoms are detected in a two-dimensional correlation experiment (dipolar recoupling enhanced by amplitude modulation, DREAM).

The main results of the NMR experiments are summarized in Figure 1; details are given in Figures S2–S4 in the

[*] A. K. Schütz, A. Soragni, Dr. M. Ernst, Prof. B. H. Meier
Physikalische Chemie, ETH Zürich, 8093 Zürich (Switzerland)
E-mail: beme@ethz.ch
Dr. S. Hornemann, Prof. A. Aguzzi
Institut für Neuropathologie, Universitäts-Spital Zürich
Schmelzbergstrasse, 8091 Zürich (Switzerland)
Dr. A. Böckmann
Institut de Biologie et Chimie des Protéines
UMR 5086 CNRS/Université de Lyon 1
7 passage du Vercors, 69367 Lyon (France)
E-mail: a.bockman@ibcp.fr

[**] This work was supported by the ETH Zurich, the Swiss National Science Foundation (Grant 200020_124611), the CNRS, and the Agence Nationale de la Recherche (ANR-07-PCVI-0013-03, ANR-06-BLAN-0266, ANR-PCV08 321323, and ANR08-PCVI-0022-02). We also acknowledge support from the European Commission under the Seventh Framework Programme (FP7), contract Bio-NMR 261863.

Supporting information for this article is available on the WWW under http://dx.doi.org/10.1002/anie.201008276.

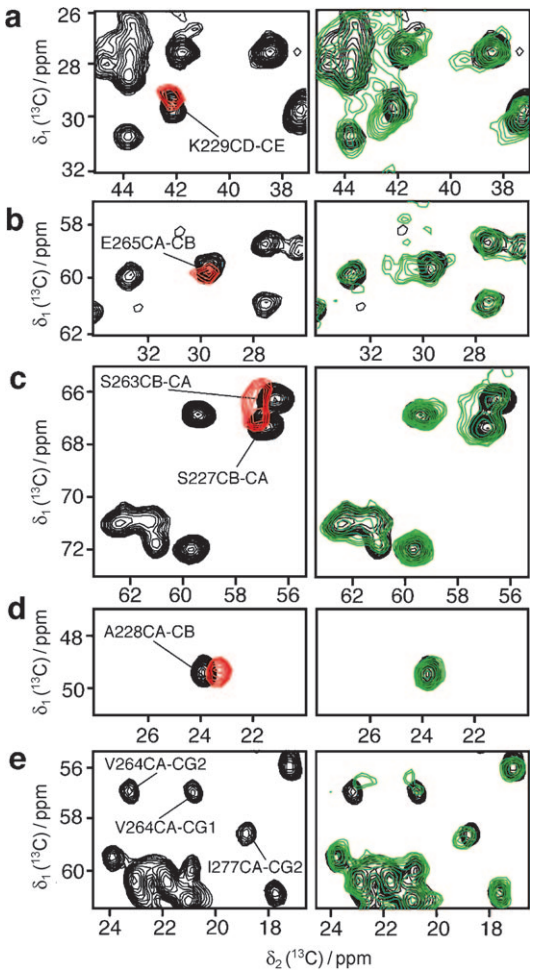

Figure 1. Left: DREAM PT spectra of Congo red bound, fully deuterated HET-s(218–289) fibrils are shown in red contours. The black contours correspond to the PDSD spectra of the control, uniformly labeled untreated fibrils. Right: PDSD spectra of Congo red bound fibrils are shown in green contours. Differences between the green and black spectra indicate CSPs. Cross-peaks discussed in the text are labeled. The PT spectrum is a difference spectrum to compensate for the background arising from imperfect deuteration (see the Supporting Information). Full spectra are shown in Figures S2 and S4, experimental parameters are given in Table S2. The symmetric cross-peaks are displayed in Figure S6.

Supporting Information. Regions of interest from the difference PT spectra are shown as red contours in the left side of Figure 1. Here we see the few but strong PT peaks plotted on top of the PDSD reference spectrum of unstained fibrils (black). Strong polarization transfer is detected from Congo red to residues S227, A228, K229, S263, and E265. No other residues obtain polarization from Congo red, as is evident in the full spectrum shown in Figure S4 in the Supporting Information. This indicates that the binding is highly specific.

The CSP effects for the same spectral regions are shown on the right side of Figure 1. First, it should be emphasized that most CSPs between stained fibrils (green contours) and the control (black contours) are small,[16] indicating that the amyloid core structure does not change upon ligand binding. Nevertheless, noteworthy CSPs and line broadenings are observed for nearly all residues with PT, i.e., for K229 Cδ–Cε (Figure 1a, right), E265 Cβ–Cα (Figure 1b), and S227/S263 Cα–Cβ (Figure 1c), and also for the adjacent V264 residue (Figure 1e). Three additional CSPs, outside the core, were detected at A248, A249, and V245 (Figure S2), which we attribute to an additional binding site not relevant to birefringence (see below). Since other Ser and Thr Cα–Cβ correlations show excellent agreement between the spectra of Congo red bound and free fibrils, temperature and pH effects can be ruled out.

The nuclei with CSP or PT upon Congo red binding are highlighted in the HET-s(218–289) structure[4b] in Figure 2. These residues appear clustered in the vicinity of the two-residue arc connecting β-sheets β1a/β1b and β3a/β3a.[4b] Residues S227, K229, S263, and E265 are surface exposed. Thus, we can dismiss an intercalation of Congo red between the turns of the β solenoid because this geometry would lead to contacts less than 4 Å between the Congo red protons and virtually all residues of the hydrophobic protein core, which would then show PT cross peaks. The experimental findings are, therefore, compatible only with a geometry in which the Congo red molecules are aligned with their long axis parallel to the fibril axis. The distance between K229 of protein monomers i and $i+2$ is on average 19 Å, close to the 20 Å distance of the two sulfonate groups in Congo red. It is noteworthy that neither CSP nor PT is detected for other lysines in the protein (K218, K270, K284, of which K270 is

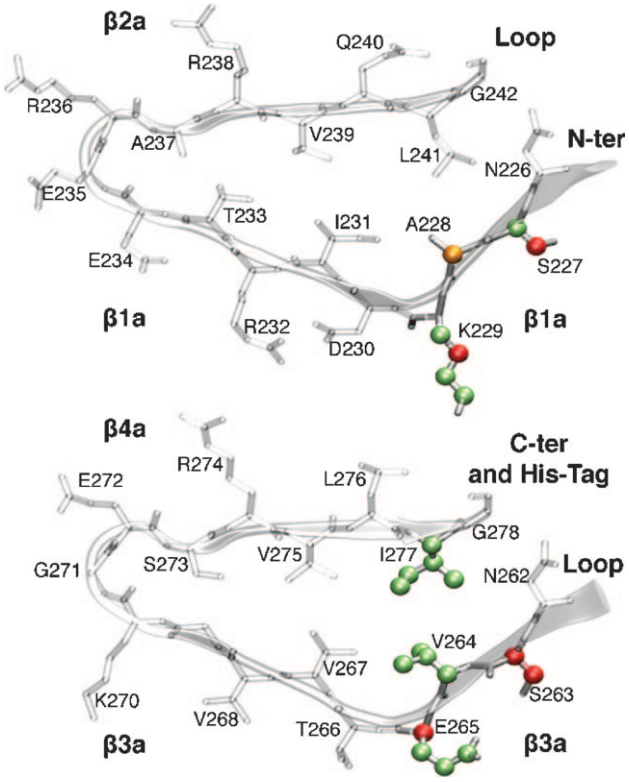

Figure 2. Summary of NMR data on Congo red binding mapped onto the core of HET-s(218–289) amyloid (PDB code 2RNM). Red spheres denote nuclei with significant CSP effects combined with PT from the ligand, orange spheres nuclei with PT only, green spheres nuclei with CSPs only.

also located in a β-sheet). This not only indicates that the interaction is highly specific, but also rules out the geometrically feasible attachment of Congo red with its long axis perpendicular to the fibril axis, that is, by interaction with the two sulfonate groups to K229 and K270 of two adjacent β-strands.

The data from CSP and PT experiments can be translated into distance restraints and be used as input for docking calculations (for a list of all restraints see Table S1.) Using the program HADDOCK,[17] semiflexible fibril side chains, and a fully flexible ligand molecule, we found the docking geometry shown in Figure 3 (PDB code: 2LBU). The Congo red molecule is embedded in a groove whose bottom is formed by

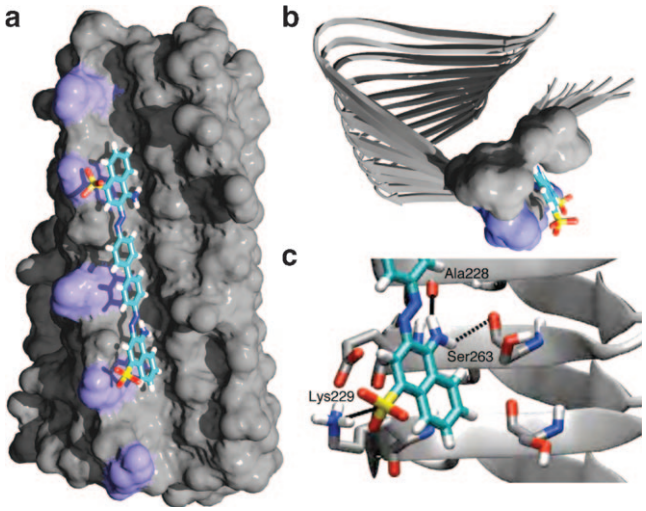

Figure 3. Structure of Congo red docked to HET-s(218–289). a) Side view of the complex. The key residue for binding, K229, is marked in purple. b) Top view showing how Congo red enters the pronounced groove formed by K229/E265 and S227/S263 (shown in surface representation). c) Hydrogen bonds between Congo red and the fibril backbone and between the electrostatic anchor and K229.

the surface of β-sheets 1a and 3a and lined by K229/E265 on one side and by S227/S263 on the other. The dye molecule is oriented with the long axis parallel to the fibril axis and the plane radial to the fibril core. The negative charges from the ligand's sulfate groups point away from the fibril surface and are in close contact (≈ 2.6 Å) with two K229 ε-amino groups (Figure 3). The Congo red molecule thus has a twofold electrostatic anchor to the i and $i+2$ HET-s(218–289) molecules. The Congo red amino groups point towards the HET-s(218–289) surface and form hydrogen bonds with accessible carbonyl groups of the fibril backbone including, over different HADDOCK ensembles, S227, A228, S263, and V264 (Figure 3c, Table S3). The model of the bound complex as obtained by HADDOCK docking is favorable in terms of van der Waals interactions (-44 ± 2 kcal mol^{-1}), electrostatic interactions (-166 ± 13 kcal mole^{-1}), and hydrogen bonds between the ligand's functional groups and the fibril surface. The torsion angle about the biphenyl bond in Congo red is reported to be apprximately 40° in the gas phase and 20–30° in solution.[18] In our docking model, this angle is consistently found to be close to planar (5 ± 3° in the ten most favorable HADDOCK structures), which can explain the redshift of the absorbance maximum upon fibril binding.[6d] If every binding site were occupied in this model, the binding stoichiometry would be one Congo red molecule per three fibril monomers (see the Supporting Information).

In summary, our experimental findings demonstrate that Congo red binds highly specifically to HET-s(218–289) fibrils along a groove running roughly parallel to the fibril axis (Figure 3). The binding site features a repetition of positively charged amino acid residues (here Lys) on the surface with a spacing of 9.5 Å defined by the cross-β arrangement of the backbone. The observed binding site distinguishes itself from other possible binding sites—including another Lys pattern with the same spacing—by the existence of a pronounced groove parallel to the fibril long axis offering the possibility of forming hydrogen bonds to the protein backbone (Figure 3c). The other lysine residue, K270, features a much less approachable backbone.

These observations lead to the testable hypothesis that a point mutation at K229 would seriously interfere with Congo red staining. Indeed, while the wild-type fibrils show pronounced birefringence upon Congo red binding, staining is weak and birefringence practically absent for the K229A mutant (Figure 4). NMR spectra (Figure S5 in the Supporting Information) clearly demonstrate that, while the structure of the fibril is virtually identical for the mutant as verified by the highly conserved chemical shifts, CSPs are absent, confirming the results from microscopy. Other mutants, which form amyloid fibrils visible under the electron microscope, were tested, namely Q240A, L241A, R238A, and V267A; these

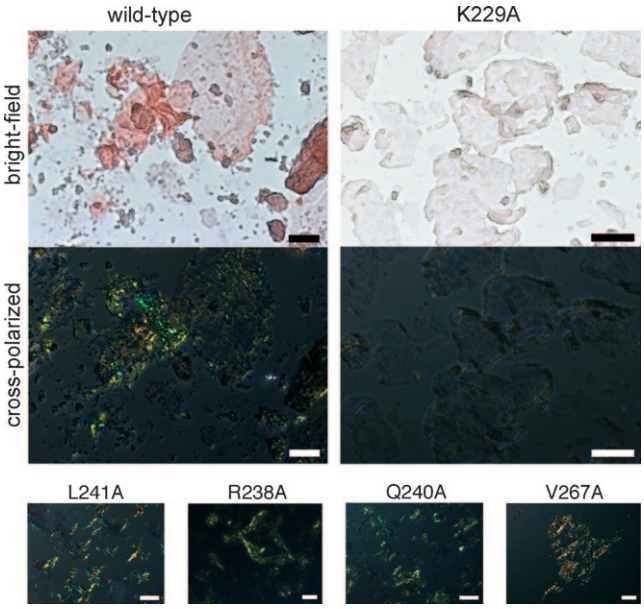

Figure 4. Comparison of Congo red staining for the different fibrils. Wild-type HET-s(218–289) is stained by Congo red and shows apple-green birefringence in polarized light. The K229A mutant stains only slightly and does not show birefringence in contrast to the wild-type and the L241A, R238A, Q240A, and V267A mutants. All scale bars are 100 μm.

mutants do not interfere with birefringence (Figure 4). As the K229A mutation did not alter the structure of the amyloid fibrils, the absence of congophilia in the fibrillogenic HET-s(218–289) lysine mutant points to a remarkable false-negative result of Congo red staining: the K229A mutant forms an amyloid and does not show birefringence. The weaker binding site at A248, A249, and V245, still present in the mutant, is therefore not important for birefringence.

Yet congophilia continues to represent the diagnostic "gold standard" for mammalian amyloidoses and many disease-related amyloids test positive. Ladders of solvent-exposed positively charged side chains, a necessary but not a sufficient condition for the congophila of HET-s(218–289), were identified in the published structural models for aβ,[19] for example. The presence of additional features identified here, namely a surface groove and the possibility of hydrogen bonding in these amyloids, is, in the absence of atomic-resolution structures, uncertain. Interestingly, bovine spongiform encephalopathy (BSE) does not typically exhibit congophilic aggregates in cows, but does so upon transmission to mice[20] and in those cases of BSE that have been singled out as "bovine amyloidotic spongiform encephalopathy (BASE)".[21] These classifications may deserve critical review in the light of our finding that the congophilia of the HET-s(218–289) amyloid can be ablated with no significant impact on the overall structure of the amyloid. Consequently, the striking findings described here raise the question whether unrecognized "congophobic" amyloidoses might underlie many more protein-misfolding diseases than is currently realized.

The methodology introduced here is also applicable to other ligands and fibrils, as well as to the characterization of small-molecule binding to insoluble proteins in general. Notably, our protocol works with unlabeled ligands, making the often-tedious ligand labeling unnecessary and facilitating screening with ligand libraries. Ultimately, detailed information on the interaction of small molecules with this pharmacologically relevant class of proteins should fertilize the development of improved amyloid markers, as well as drugs that interfere with fibril formation or stability to ultimately prevent and cure this class of diseases.

Experimental Section

The stained NMR samples were produced by incubating 15 mg of fibrillized protonated protein, prepared as described previously,[4b] with a tenfold molar excess of Congo red disodium salt (CR; CALBIOCHEM, catalog number 234610) in deionized water for five days with gentle shaking at room temperature. The unbound CR was subsequently washed off by five cycles of centrifugation (at 4000 rpm, 3220 g) and resuspension of the pellet in 50 mL of deionized water. The supernatant after the last centrifugation was colorless. All samples were resuspended in 50 mM Tris-HCl buffer at pH 7.4. Finally, the fibrils were centrifuged (1 h at ≈154000 g) into 2.5 mm Varian rotors using an ultracentrifuge.[22] A reference sample without CR was prepared and treated identically through all steps, except the CR addition.

A second set of samples was prepared with triply labeled [^{2}H,^{13}C,^{15}N] fibrils for polarization-transfer (PT) measurements. After desalting, the monomer solution was lyophilized, resuspended in D_2O (99.85% D_2O, EURISO-TOP), and immediately lyophilized again. After a second resuspension in D_2O, the solution was adjusted to pH 7.4 (uncompensated for effects of deuteration on pH measurements) using 3 M Tris in D_2O. The fibrillization occurred overnight while the sample was shaken gently at room temperature. The batch was separated in two, and half of it was allowed to bind a tenfold molar excess of CR disodium salt with natural isotopic abundance for five days. Subsequently both preparations were washed in D_2O five times. The fibrils were filled into 3.2 mm Bruker rotors using an ultracentrifuge (1 h at ≈107000 g), in this case without pH-stabilizing buffer to avoid proton contamination. The reference sample was treated identically at all times (except the addition of CR).

Received: December 30, 2010
Revised: March 3, 2011
Published online: May 17, 2011

Keywords: amyloids · Congo red · prions · proteins · structure elucidation

[1] F. Chiti, C. M. Dobson, *Annu. Rev. Biochem.* **2006**, *75*, 333.
[2] S. Maji, M. Perrin, M. Sawaya, S. Jessberger, K. Vadodaria, R. Rissman, P. Singru, K. Nilsson, R. Simon, D. Schubert, D. Eisenberg, J. Rivier, P. Sawchenko, W. Vale, R. Riek, *Science* **2009**, *323*, 328.
[3] P. Westermark, M. D. Benson, J. N. Buxbaum, A. S. Cohen, B. Frangione, S.-I. Ikeda, C. L. Masters, G. Merlini, M. J. Saraiva, J. D. Sipeo, *Amyloid* **2007**, *14*, 179.
[4] a) C. Ritter, M.-L. Maddelein, A. B. Siemer, T. Lührs, M. Ernst, B. H. Meier, S. J. Saupe, R. Riek, *Nature* **2005**, *435*, 844; b) C. Wasmer, A. Lange, H. Van Melckebeke, A. B. Siemer, R. Riek, B. H. Meier, *Science* **2008**, *319*, 1523; c) H. Van Melckebeke, C. Wasmer, A. Lange, E. Ab, A. Loquet, A. Böckmann, B. H. Meier, *J. Am. Chem. Soc.* **2010**, *132*, 13765.
[5] H. Bennhold, *Muench. Med. Wochenschr.* **1922**, *69*, 1537.
[6] a) E. P. Benditt, N. Eriksen, C. Berglund, *Proc. Natl. Acad. Sci. USA* **1970**, *66*, 1044; b) H. Puchtler, F. Sweat, M. Levine, *J. Histochem. Cytochem.* **1962**, *10*, 355; c) P. Frid, S. V. Anisimov, N. Popovic, *Brain Res. Rev.* **2007**, *53*, 135; d) M. Groenning, *J. Chem. Biol.* **2009**, *3*, 1.
[7] M. Higuchi, N. Iwata, Y. Matsuba, K. Sato, K. Sasamoto, T. Saido, *Nat. Neurosci.* **2005**, *8*, 527.
[8] a) A. Lorenzo, B. A. Yankner, *Proc. Natl. Acad. Sci. USA* **1994**, *91*, 12243; b) I. Sánchez, C. Mahlke, J. Yuan, *Nature* **2003**, *421*, 373; c) C. Lendel, C. W. Bertoncini, N. Cremades, C. A. Waudby, M. Vendruscolo, C. M. Dobson, D. Schenk, J. Christodoulou, G. Toth, *Biochemistry* **2009**, *48*, 8322.
[9] W. E. Klunk, J. W. Pettegrew, D. J. Abraham, *J. Histochem. Cytochem.* **1989**, *37*, 1273.
[10] a) P. Ladewig, *Nature* **1945**, *156*, 81; b) A. J. Howie, D. B. Brewer, *Micron* **2009**, *40*, 285.
[11] W. Klunk, M. Debnath, A. Koros, J. Pettegrew, *Life Sci.* **1998**, *63*, 1807.
[12] D. Carter, K. Chou, *Neurobiol. Aging* **1998**, *19*, 37.
[13] a) H. Inouye, J. Nguyen, P. Fraser, L. Shinchuk, *Amyloid* **2000**, *7*, 179; b) F. Cavillon, A. Elhaddaoui, A. Alix, S. Turrell, M. Dauchez, *J. Mol. Struct.* **1997**, *408–409*, 185.
[14] W. Jahnke, H. Widmer, *Cell. Mol. Life Sci.* **2004**, *61*, 580.
[15] M. Etzkorn, A. Böckmann, A. Lange, M. Baldus, *J. Am. Chem. Soc.* **2004**, *126*, 14746.
[16] a) P. C. A. van der Wel, J. R. Lowandowski, R. G. Griffin, *Biochemistry* **2010**, *49*, 9457; b) A. Lange, K. Giller, S. Hornig, M. F. Martin-Eauclaire, O. Pongs, S. Becker, M. Baldus, *Nature* **2006**, *440*, 959; c) L. B. Andreas, M. T. Eddy, R. M. Pielak, J. Chou, R. G. Griffin, *J. Am. Chem. Soc.* **2010**, *132*, 10958.
[17] S. J. de Vries, M. van Dijk, A. M. Bonvin, *Nat. Protoc.* **2010**, *5*, 883.

[18] D. Barich, R. Pugmire, D. Grant, R. Iuliucci, *J. Phys. Chem. A* **2001**, *105*, 6780.
[19] A. Petkova, W. Yau, R. Tycko, *Biochemistry* **2006**, *45*, 498.
[20] C. J. Sigurdson, K. Peter, R. Nilsson, S. Hornemann, G. Manco, M. Polymenidou, P. Schwarz, M. Leclerc, P. Hammarstrom, K. Wuthrich, A. Aguzzi, *Nat. Methods* **2007**, *4*, 1023.
[21] C. Casalone, G. Zanusso, P. Acutis, S. Ferrari, L. Capucci, F. Tagliavini, S. Monaco, M. Caramelli, *Proc. Natl. Acad. Sci. USA* **2004**, *101*, 3065.
[22] A. Böckmann, C. Gardiennet, R. Verel, A. Hunkeler, A. Loquet, G. Pintacuda, L. Emsley, B. H. Meier, A. Lesage, *J. Biomol. NMR* **2009**, *45*, 319.

